We are IntechOpen, the world's leading publisher of Open Access books Built by scientists, for scientists

4,800
Open access books available

122,000
International authors and editors

135M
Downloads

Our authors are among the

154
Countries delivered to

TOP 1%
most cited scientists

12.2%
Contributors from top 500 universities

CLARIVATE ANALYTICS BOOK CITATION INDEX INDEXED

WEB OF SCIENCE™

Selection of our books indexed in the Book Citation Index in Web of Science™ Core Collection (BKCI)

Interested in publishing with us?
Contact book.department@intechopen.com

Numbers displayed above are based on latest data collected.
For more information visit www.intechopen.com

11

Integrated-Optic Circuits for Recognition of Photonic Routing Labels

Nobuo Goto, Hitoshi Hiura, Yoshihiro Makimoto and Shin-ichiro Yanagiya
The University of Tokushima
Japan

1. Introduction

An optical fiber provides enormous capacity of more than tens terabits per second for transmission in photonic networks, whereas packet processing in network nodes will become a bottleneck for large-capacity networking. For realization of large-capacity and high-speed photonic networks, fast optical processing without conversion to electric signal is preferable (Seo et al., 1996; Blumenthal et al., 2000).

Photonic routing has been attracting much interest to overcome the bottleneck of routing function in high-speed networks. In particular, photonic label routing network is expected to provide fast routing of packets at high-bit rate with simple processing. So far, various methods for optical label encoding and decoding have been studied (Kitayama et al., 2000; Goto & Miyazaki, 2005). As one of the nature of light, phase of coherent light has been effectively used in various optical systems, where the interference behavior between multiple signals can be easily used. Using this feature, label recognition techniques have been investigated for photonic routers based upon optical code correlation. However, most of the proposed systems cannot recognize all the binary codes because only the codes that provide enough discrimination between auto-correlation and cross-correlation can be recognized. In addition, in most systems, each optical integrated circuit recognizes only one label (Wada et al., 1999; Takiguchi et al., 2002). Therefore, it is necessary to prepare multiple correlators at each node in order to recognize all the routing labels. On the contrary, for processing of multiple labels, Moriwaki et al. (Moriwaki et al., 2005) and Cincotti (Cincotti, 2004) proposed label recognition systems where self-routing architecture was employed for phase-shift-keying (PSK) labels. On the other hand, Glesk et al. reported a demonstration of optical multiple label recognition for on-off keying (OOK) codes at 250Gbit/s using a self-routing scheme (Glesk et al., 1997). The self-routing of label data stream for label recognition is one of promising methods in label decoding system.

Hiura & Goto proposed a label recognition system for OOK labels (Hiura et al, 2005; Hiura et al, 2007a). Although the proposed system can recognize all the binary-code labels, the system requires many optical switches controlled by optical signals. A similar system was also reported by Kurumida et al. (Kurumida et al., 2006). On the other hand, Hiura et al. also proposed an all-optical passive label recognition system for all the binary codes in binary PSK (BPSK) format (Hiura et al., 2006; Hiura et al., 2007b). The label recognition system consists of a tree-structure connection of passive waveguide components named as

Source: Advances in Optical and Photonic Devices, Book edited by: Ki Young Kim,
ISBN 978-953-7619-76-3, pp. 352, January 2010, INTECH, Croatia, downloaded from SCIYO.COM

asymmetric X-junction coupler (Izutsu et al., 1982; Burns & Milton, 1975; Burns & Milton, 1980), and time gates. The asymmetric X-junction coupler provides a function of wave coupling according to the phase relation between the two incident waves. The asymmetric X-junction coupler has an advantage that the wave coupling behavior does not depend on wavelength because the wave coupling utilizes an adiabatic wave coupling along the X-junction. This feature cannot be obtained with other devices such as 3-dB directional couplers or multi-mode interference (MMI) couplers.

The number of represented labels in PSK format can be increased by employing multiple phases such as four phases as quadri-PSK (QPSK). Optical circuits for detecting QPSK signal have been investigated for receivers in communication systems (Renaudier et al., 2008). When QPSK labels are introduced in label routing system, optical processing of the QPSK labels is required. We have proposed a label recognition circuit for QPSK labels (Makimoto et al., 2008; Makimoto et al, 2009a). The circuit consists of the asymmetric X-junction couplers, Y-junctions and 3-dB directional couplers.

In this article, we describe the principle of label recognition for BPSK and QPSK coded labels in the self-routing scheme. The operation of the label recognition with optical integrated circuits are confirmed by finite-difference beam propagation method (FD-BPM).

2. Photonic label router

Optical labels are used as a routing information in photonic label switching network as shown in Fig.1. A label is attached to the incident packet at an edge router. The label is used to forward the packet to another edge router which is connected to the destination of the packet. At a node, routing switches are controlled according to the label information by referring to a routing table. At first, the label has to be analyzed to find the destination information. Therefore, the label has to be inspected whether the label matches with any of the all labels at the routers.

If the network is designed in a hierarchical structure so that a router at a node in a sub-network is required to find only the packets destined to the sub-network, it is not required for the router to resolve all the labels. Therefore, it depends on the network architecture and routing protocol whether all the labels have to be resolved or only a part of the labels are required to be resolved.

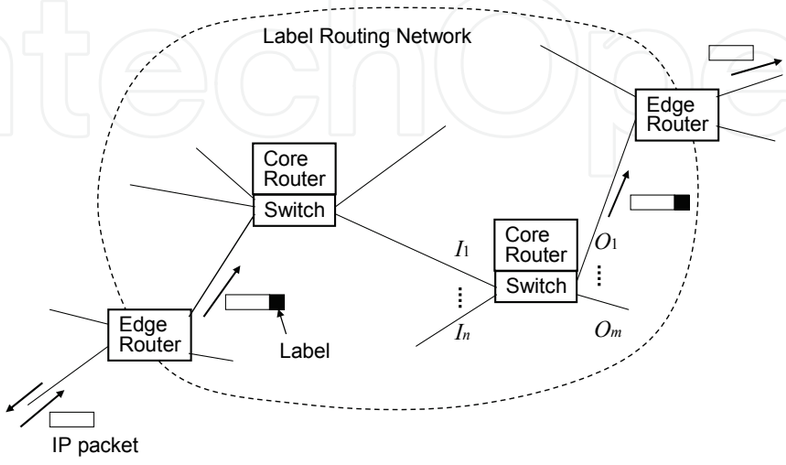

Fig. 1. Label routing network.

3. Optical label and its recognition

Various methods have been investigated to represent routing label information as optical signals, which include coding of the labels in time-domain, in spectral domain, and in their combination. Here we consider time sequential coded pulse train in BPSK and QPSK modulation formats. In these pulses encoded in phase, a reference signal is required to identify their absolute phase. Although differential PSK formats can be alternatives that do not require the reference phase signal, we introduce a reference pulse in advance of the pulses representing an address to identify general PSK address as shown in Fig.2. The electric field of the optical pulse train of an (N+1)-bit label is written as

$$E_{label}(t) = \sum_{i=0}^{N} f_0(t - i\Delta t) e^{j\phi_i} e^{j\omega(t-i\Delta t)}, \tag{1}$$

where $f_0(t)$ denotes the envelope of a pulse with the angular frequency ω, the phase ϕ_i and the pulse period Δt. j is the imaginary symbol of $j = \sqrt{-1}$. The phase is 0 or π in BPSK labels and 0, π/2, π or 3π/2 in QPSK labels. The phase ϕ_0 is assumed to be 0 as the reference pulse, named as identifying (ID) bit in our self-routing label recognition systems. The other phases ϕ_i, i=1,…, N, represent the address.

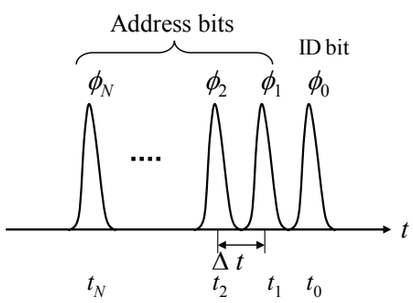

Fig. 2. Label structure in PSK format.

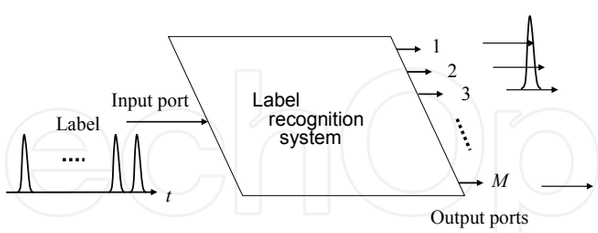

Fig. 3. Label recognition system.

The label recognition is performed by forwarding the ID-bit pulse to an output port corresponding to the destination of the address as shown in Fig.3. The number of the output ports M corresponds to the number of all the coded address, that is, M=2^N and 4^N for BPSK and QPSK codes, respectively. Since all the bits of the label arrive sequentially, we employ a processing circuit to extend all the bits in parallel at a specific time as shown in Fig.4. Equally-divided pulse trains are sent to the input ports of the label recognition circuit through delay elements. The incident electric field of the optical signal to input port I_k, k=1,…,N+1, is delayed by (k-1)Δt as given by

$$E_{label}^{(k)}(t) = \frac{1}{\sqrt{N+1}} \sum_{i=0}^{N} f_0(t-(i+k-1)\Delta t) e^{j\phi_i} e^{j\omega[t-(i+k-1)\Delta t]}. \quad (2)$$

At time t_c, all the (N+1)-bit pulses simultaneously enter to the input ports.

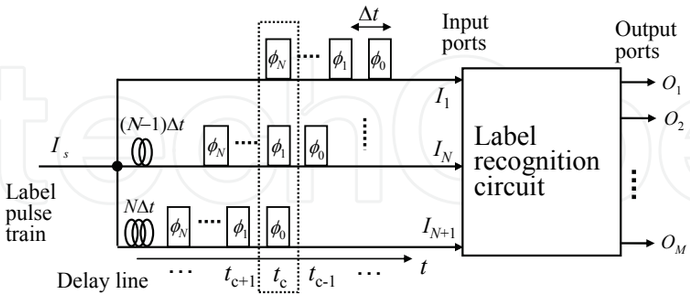

Fig. 4. Label recognition with serial-to-parallel conversion as a pre-processing.

Figure 5 shows the principle of label recognition by self-routing manner. Each bit of the address represents the number of M_0=2 and 4 for BPSK and QPSK, respectively. The nth-stage circuit module forwards the ID bit pulse to the output port corresponding to the nth address bit by using the nth address bit pulse as the control signal. Consequently, the ID bit pulse appears at the destination port among the $M=M_0{}^N$ output ports in the Nth-stage.

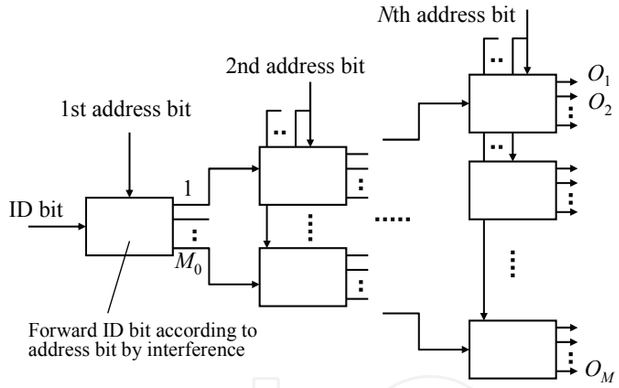

Fig. 5. Tree-structure circuit for label recognition by self-routing manner.

4. Basic devices for recognition circuits

Proposed label recognition circuits consist of passive waveguide devices shown in Fig.6. A 3-dB directional coupler shown in (a) is used to couple the optical incident waves into two output waves. The electric field of the input and output waves, $E_{in}{}^{(i)}$ and $E_{out}{}^{(i)}$, i=1,2, are related, by eliminating the common phase shift along the propagation, as

$$\begin{pmatrix} E_{out}^{(1)} \\ E_{out}^{(2)} \end{pmatrix} = \frac{1}{\sqrt{2}} \begin{pmatrix} 1 & -j \\ -j & 1 \end{pmatrix} \begin{pmatrix} E_{in}^{(1)} \\ E_{in}^{(2)} \end{pmatrix}. \quad (3)$$

When an optical wave is incident in only one of the waveguide, the wave is equally divided. The output fields, however, have a phase difference of $\pi/2$. A Y-junction shown in (b) also divides an optical input wave equally into two output ports as expressed by

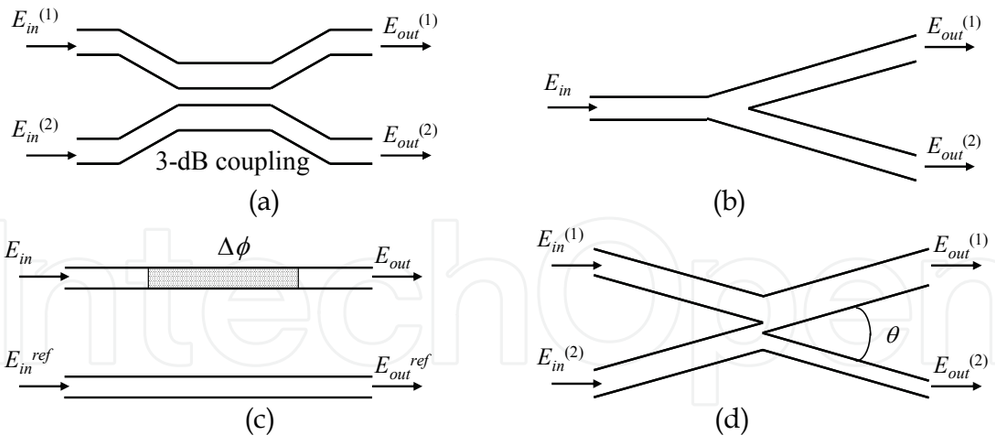

Fig. 6. Basic passive elements for label recognition circuits.

$$\begin{pmatrix} E_{out}^{(1)} \\ E_{out}^{(2)} \end{pmatrix} = \frac{1}{\sqrt{2}} \begin{pmatrix} 1 \\ 1 \end{pmatrix} E_{in}. \tag{4}$$

The two output waves have the same phase. A phase shifter shown in (c) shifts the phase with regard to the reference waveguide. The input-output relation is given by

$$\begin{pmatrix} E_{out} \\ E_{out}^{ref} \end{pmatrix} = \begin{pmatrix} e^{j\Delta\phi} & 0 \\ 0 & 1 \end{pmatrix} \begin{pmatrix} E_{in} \\ E_{in}^{ref} \end{pmatrix}. \tag{5}$$

An asymmetric X-junction coupler shown in (d) is the device whose input and output are a symmetric Y-junction and an asymmetric Y-junction, respectively (Izutsu et al., 1982). When two waves are incident in phase, the output is obtained only at the wider-waveguide port. On the contrary, when two waves are incident in opposite phase, the output is at the narrower waveguide. This input-output relation is given by

$$\begin{pmatrix} E_{out}^{(1)} \\ E_{out}^{(2)} \end{pmatrix} = \frac{1}{\sqrt{2}} \begin{pmatrix} 1 & 1 \\ -1 & 1 \end{pmatrix} \begin{pmatrix} E_{in}^{(1)} \\ E_{in}^{(2)} \end{pmatrix}. \tag{6}$$

It is noted that the output fields have a phase difference of π. The angle θ and the waveguide asymmetry have to be properly designed to realize the ideal routing characteristics. The phenomenon of optical coupling along an asymmetric Y-branch is evaluated by the coupled mode theory (Burns & Milton, 1975; Burns & Milton, 1980). A parameter Ψ to characterize the coupling phenomenon is defined by

$$\Psi = \frac{N_w - N_n}{\theta\sqrt{(N_w + N_n)^2/4 - n_s^2}}, \tag{7}$$

where n_s is the refractive index of the cladding region, N_w and N_n are the effective indices of the wide and narrow waveguides, respectively, θ is the branching angle. The ideal function as given by eq.(6) is expected to be realized in the asymmetric X-junction coupler when $\Psi > 0.44$.

5. BPSK label recognition

The asymmetric X-junction coupler has a function to discriminate the phase of the incident wave in BPSK format. A cascaded connection of the asymmetric X-junction couplers in a tree-structure shown in Fig. 7 can identify two-bit addresses. The symbol X_{ij} denotes an asymmetric X-junction coupler at the ith stage. Each of the waveguides numbered by 3 and 4 corresponds to the wider and the narrower waveguide, respectively. The input and output fields are related as

$$\begin{pmatrix} E_{out}^{(1)} \\ E_{out}^{(2)} \\ E_{out}^{(3)} \\ E_{out}^{(4)} \end{pmatrix} = \begin{pmatrix} 1 & -1 & \alpha_2 \\ -1 & 1 & \alpha_2 \\ 1 & 1 & \alpha_2 \\ -1 & -1 & \alpha_2 \end{pmatrix} \begin{pmatrix} E_{in}^{(1)} \\ E_{in}^{(2)} \\ E_{in}^{(3)} \end{pmatrix}, \tag{7}$$

where α_2 is an amplification coefficient of the amplifier placed at input port I_3. We consider two cases having different value of α_2. First we consider the case of α_2=1. When optical two-bit BPSK pulse train is incident, the normalized intensity of the pulse trains appears from four output ports as shown in Fig.8. The maximum output is found at time t_c , and four

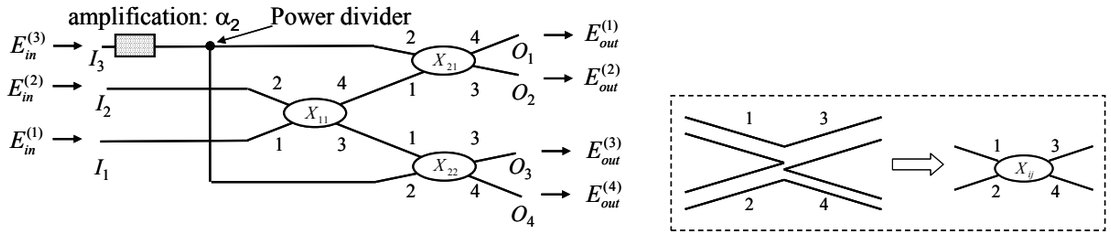

Fig. 7. BPSK label recognition circuit for label length three.

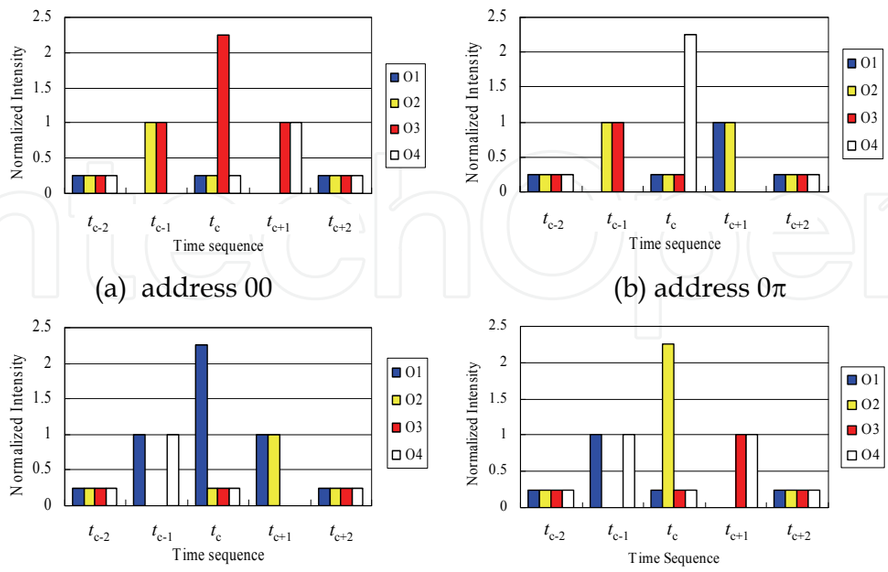

(a) address 00 (b) address 0π

(c) address π0 (d) address ππ

Fig. 8. Time sequential output intensity for four addresses with the circuit of α_2=1.

different addresses have the peak intensity at their corresponding output port. The contrast ratio of the peak intensity to the second largest intensity at time t_c is 9. Since the inputs to the second asymmetric X-junction couplers, X_{2j}, j=1,2, have different intensities, the output from the port whose paired port has the maximum intensity has a non-zero output.

Next, we consider the case of α_2=2. The pulse train from four output ports appear as shown in Fig.9. In this case, the input intensities to the X-junction coupler that has the maximum output are equal, and no output at the paired port. The contrast ratio of the maximum intensity to the second intensity at time t_c is decreased to 4.

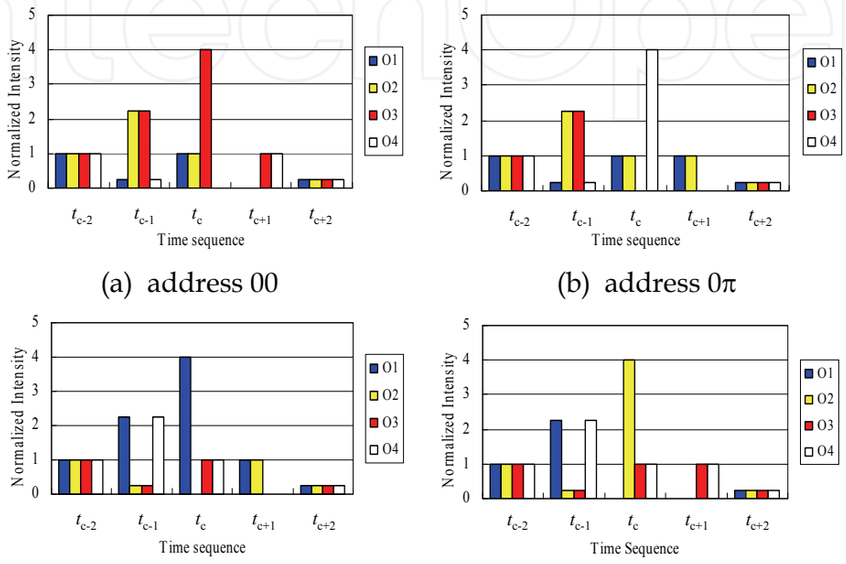

(a) address 00 (b) address 0π

(c) address π0 (d) address ππ

Fig. 9. Time sequential output intensity for four labels with the circuit of α_2=2.

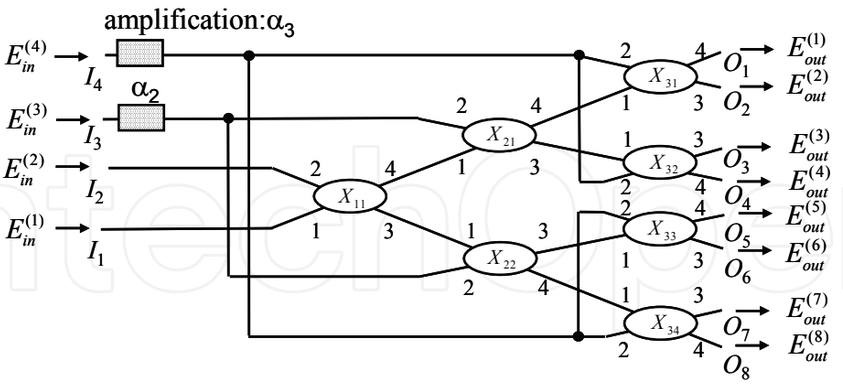

Fig. 10. BPSK label recognition circuit for label length four.

The circuit shown in Fig.7 can be scaled up for label length four as shown in Fig.10. The pulse train coupled in the input port I_4 is amplified by a factor α_3 and divided into four pulse trains for the third-stage X-junction couplers. The contrast ratio of the maximum output intensity to the second largest intensity is decreased as shown in Fig.11. It is found that for the case of α_m=1, m=2,…, N-1, 7-bit addresses can be recognized with the contrast ratio of 2.5[dB]. On the contrary, for the case of α_m=2^{m-1}, even 4-bit addresses are difficult to

recognize. However, by regarding the null-output port as the port indicating the address, the address can be recognized. The maximum output intensity, $P_{IC,max}$ and the second smallest output intensity $P_{IC,min}$ are plotted in Fig.12. The decrease of $P_{IC,min}$ and the increase of $P_{IC,max}$ limit the recognized address bits. These values are -12dB and 18dB, respectively, for 5-bit addresses.

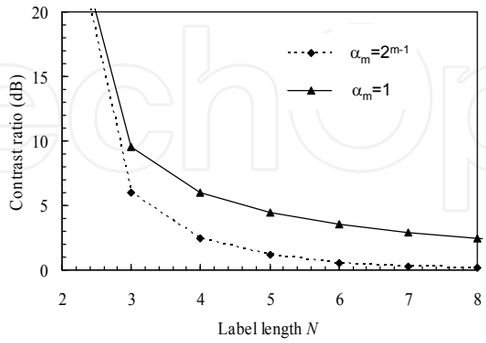

Fig. 11. Comparison of the contrast ratio of the outputs for two cases.

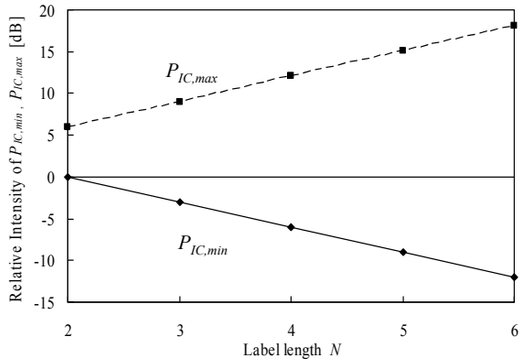

Fig. 12. Relative output intensity of the maximum output and the second smallest output for the second case of $\alpha_m=2^{m-1}$.

The recognition characteristics were verified with computer simulation by FD-BPM. A two-dimensional model of the 2-stage device for label length three is shown in Fig.13. The waveguide circuit is assumed to be made of slab-type Ge-doped silica waveguides. The refractive indices of the core and the cladding regions are 1.461 and 1.450, respectively, at wavelength 1550nm. The core width is W=3μm for the input waveguides 1 and 2, W_3=3.4μm for the wider waveguide 3 and W_4=2.6μm for the narrower waveguide 4. The effective indices are calculated to be N_w=1.4560 and N_n=1.45472 at λ=1550 nm from the dispersion equation of guided waves. The crossing angle θ is 0.004rad. The parameter Ψ of eq.(7) is then evaluated to be 2.56. This value is enough larger than 0.44 and the routing function of eq. (6) is expected.

The hatched waveguides with width W_a=2.9μm and W_b=3.1μm are introduced to compensate the path-length difference. The total device length L is 20mm. The BPM simulation was performed for TE mode. Examples of the results for address "00" and "π0" with α_2=1 are shown in Fig.14, where the intensity profiles is shown. The incident fields to

I_1, I_2 and I_3' are assumed to be e^{j0}, e^{j0} and $(1/\sqrt{2})e^{j0}$ for address "00" and e^{j0}, $e^{j\pi}$ and $(1/\sqrt{2})e^{j0}$ for address "π0", respectively. The results agree well with the theoretical analysis.

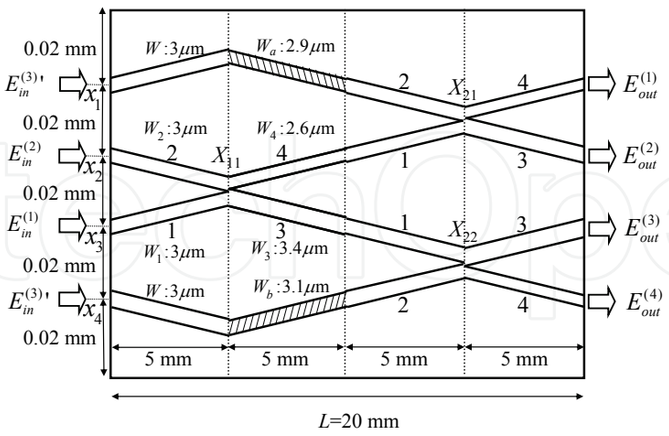

Fig. 13. Two-dimensional waveguide model for FD-BPM simulation.

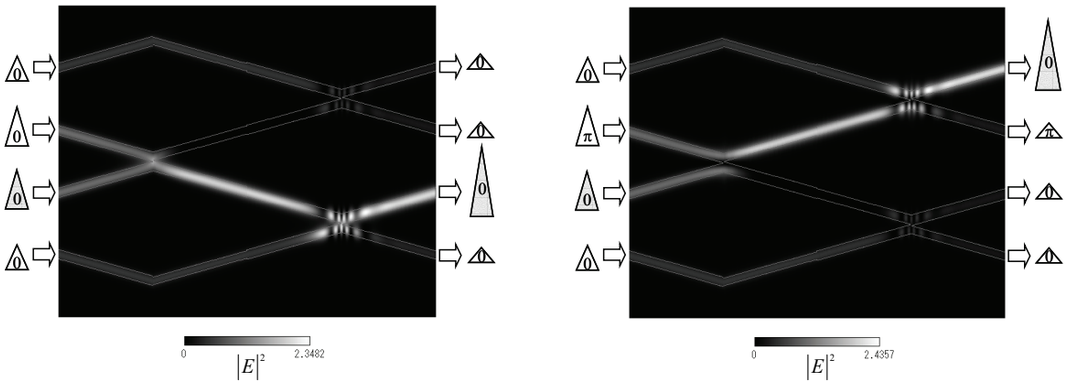

(a) "00": $(E_{in}^{(1)}, E_{in}^{(2)}, E_{in}^{(3)}') = (e^{j0}, e^{j0}, (1/\sqrt{2})e^{j0})$ (b) "π0": $(E_{in}^{(1)}, E_{in}^{(2)}, E_{in}^{(3)}') = (e^{j0}, e^{j\pi}, (1/\sqrt{2})e^{j0})$

Fig. 14. Simulation results for two different labels.

6. QPSK label recognition

By combining the basic waveguide devices shown in Fig.6, we proposed a circuit for QPSK label recognition. Figure 15 shows the basic circuit module which recognizes the phase of an incident QPSK code. This basic module is regarded as a QPSK phase recognition circuit (QPRC). The QPRC consists of a 3-dB directional coupler, two Y-junctions, and an asymmetric X-junction coupler. There are two input ports and four output ports. The electric fields of the optical signals at the output of the two Y-junctions, $E_{Y\text{-}out}^{(i)}$, i=1,…,4, are written using eqs.(3) and (4) as

$$\begin{pmatrix} E_{Y-out}^{(1)} \\ E_{Y-out}^{(2)} \\ E_{Y-out}^{(3)} \\ E_{Y-out}^{(4)} \end{pmatrix} = \frac{1}{2}\begin{pmatrix} 1 & 0 \\ 1 & 0 \\ 0 & 1 \\ 0 & 1 \end{pmatrix}\begin{pmatrix} 1 & -j \\ -j & 1 \end{pmatrix}\begin{pmatrix} E_{in}^{(1)} \\ E_{in}^{(2)} \end{pmatrix}. \tag{8}$$

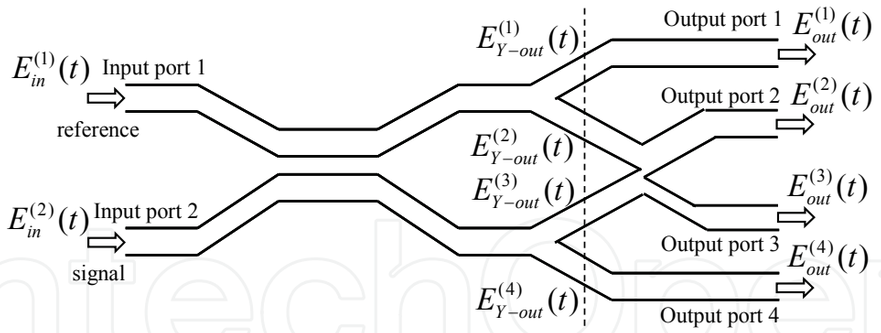

Fig. 15. Phase recognition circuit for one-bit QPSK signal.

After passing the asymmetric X-junction coupler, we obtain the output fields as

$$\begin{pmatrix} E_{out}^{(1)} \\ E_{out}^{(2)} \\ E_{out}^{(3)} \\ E_{out}^{(4)} \end{pmatrix} = \frac{1}{2}\begin{pmatrix} 1 & 0 & 0 & 0 \\ 0 & 1/\sqrt{2} & 1/\sqrt{2} & 0 \\ 0 & -1/\sqrt{2} & 1/\sqrt{2} & 0 \\ 0 & 0 & 0 & 1 \end{pmatrix}\begin{pmatrix} E_{Y-out}^{(1)} \\ E_{Y-out}^{(2)} \\ E_{Y-out}^{(3)} \\ E_{Y-out}^{(4)} \end{pmatrix} \tag{9}$$

$$= \frac{1}{2}\begin{pmatrix} 1 & -j \\ (1-j)/\sqrt{2} & (1-j)/\sqrt{2} \\ (-1-j)/\sqrt{2} & (1+j)/\sqrt{2} \\ -j & 1 \end{pmatrix}\begin{pmatrix} E_{in}^{(1)} \\ E_{in}^{(2)} \end{pmatrix} = \frac{1}{2}\begin{pmatrix} 1 & e^{j3\pi/2} \\ e^{j7\pi/4} & e^{j7\pi/4} \\ e^{j5\pi/4} & e^{j\pi/4} \\ e^{j3\pi/2} & 1 \end{pmatrix}\begin{pmatrix} E_{in}^{(1)} \\ E_{in}^{(2)} \end{pmatrix}.$$

We consider the outputs of the QPRC for each input code. We assume the reference signal $E_{in}^{(1)}(t)$ to be 1, and $E_{in}^{(2)}(t)$ to be four kinds of different phase signals as $E_{in}^{(2)}(t)$=1, j, -1, and -j, corresponding to the phase ϕ_2=0, $\pi/2$, π, and $3\pi/2$, respectively. Table 1 shows electric fields of the optical amplitudes $E_{out}^{(i)}(t)$, i=1,...,4, at the output ports. The output intensities at the output ports are plotted in Fig.16. The maximum and minimum outputs are obtained at different ports for different phases of $E_{in}^{(2)}$. Thus, the four different QPSK signals can be distinguished with this circuit by identifying the maximum output port or the minimum output port.

Now we consider the output from the QPRC in the system shown in Fig.3. The output intensities at times t_0-2Δt, t_0-Δt, t_0, t_0+Δt and t_0+2Δt are shown in Fig.17, where the phase of the incident QPSK code is assumed as ϕ_1= ϕ_2=0, that is ($E_{in}^{(1)}$, $E_{in}^{(2)}$)=(1,1). The second largest intensity at t_0-Δt is found to be 0.5625 at three output ports. Since this intensity is smaller than the second largest intensity of 0.625 at t=t_0, the maximum output port can be recognized by using a threshold device without using time-gating devices.

Input phase ϕ_2	Output amplitude			
	$E_{out}^{(1)}$	$E_{out}^{(2)}$	$E_{out}^{(3)}$	$E_{out}^{(4)}$
0	$e^{j7\pi/4}/\sqrt{2}$	$e^{j7\pi/4}$	0	$e^{j7\pi/4}/\sqrt{2}$
π	$e^{j\pi/4}/\sqrt{2}$	0	$e^{j5\pi/4}$	$e^{j7\pi/4}/\sqrt{2}$
$\pi/2$	1	$1/\sqrt{2}$	$e^{j\pi}/\sqrt{2}$	0
$3\pi/2$	0	$e^{j3\pi/2}/\sqrt{2}$	$-e^{j3\pi/2}/\sqrt{2}$	$e^{j3\pi/2}$

Table 1. Electric fields of the optical outputs for four different phase inputs.

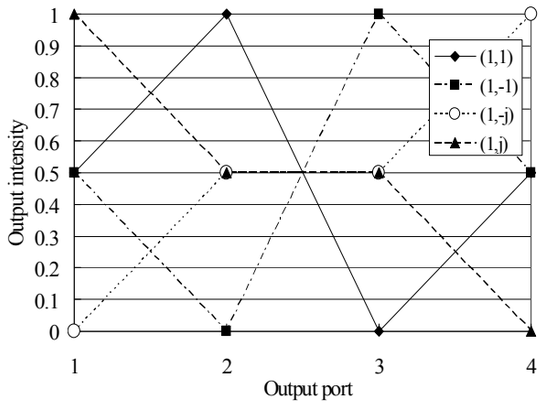

Fig. 16. Output intensities for four different phase inputs.

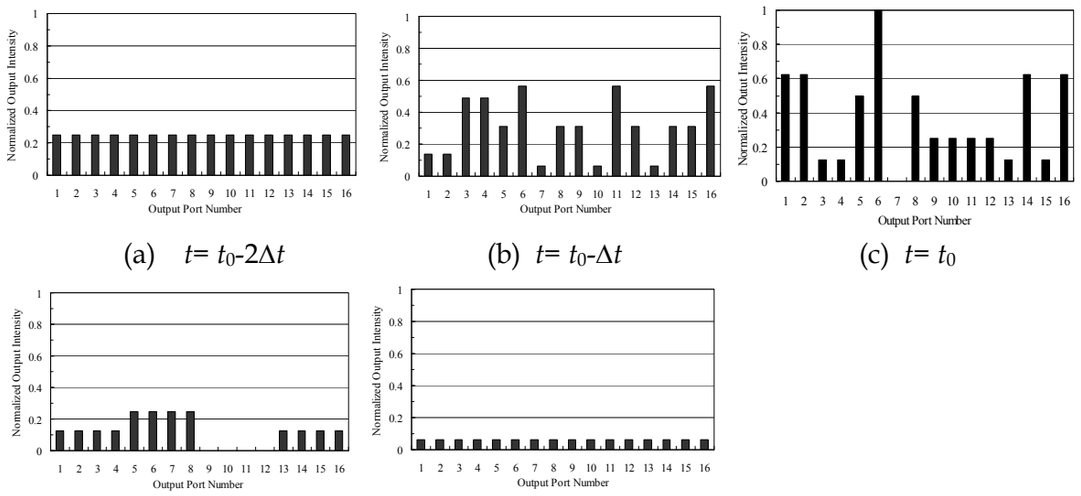

(a) $t = t_0 - 2\Delta t$ (b) $t = t_0 - \Delta t$ (c) $t = t_0$

(d) $t = t_0 + \Delta t$ (e) $t = t_0 + 2\Delta t$

Fig. 17. Output intensities for $\phi_1 = \phi_2 = 0$ at different time instances.

We confirm the principle of the operation with the QPRC module by FD-BPM simulation. The model used in the simulation is two-dimensional waveguide circuit as shown in Fig.18. Optical guided waves propagate in TE mode. The refractive indices of the core and cladding materials are assumed to be 1.461 and 1.45, respectively, at the wavelength of 1.55μm. The basic waveguide width is designed to be 3.0μm to support only the fundamental mode. The wider and narrower waveguides of the asymmetric X-junction coupler are 3.4μm and 2.6μm, respectively, with the branch angle of 0.004rad. The 3-dB directional coupler has the coupling region of 2.1818mm with the gap of 7.2μm. The total length and the width of the QPRC module is 30mm and 100μm, respectively. Figure 19 shows examples of the simulation results for two different kinds of input phases. When the two incident waves are in phase, corresponding to $(E_{in}^{(1)}, E_{in}^{(2)})=(1,1)$, the maximum signal is found at output port 2, whereas no signal is output at the output port 3 as shown in (a). When the input wave in input port 2 has the phase shifted by $\pi/2$, corresponding to $(E_{in}^{(1)}, E_{in}^{(2)})=(1,-j)$, the maximum signal is found at output port 4, whereas no signal is output at output port 1 as shown in (b).

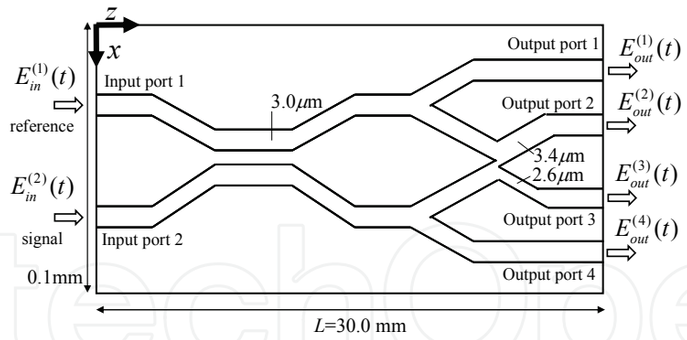

Fig. 18. Two-dimensional model of QPSK phase recogniton circuit for FD-BPM simulation.

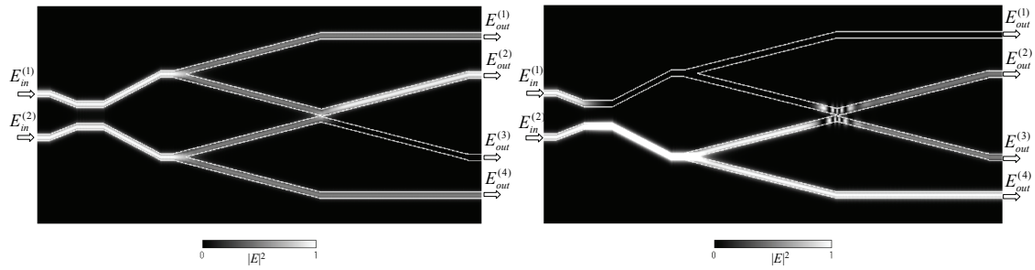

(a) $(E_{in}^{(1)}, E_{in}^{(2)})=(1, 1)$ (b) $(E_{in}^{(1)}, E_{in}^{(2)})=(1,-j)$

Fig. 19. FD-BPM simulation results for two different phase inputs.

Next, we consider a recognition circuits for a two-bit QPSK address. First, we consider a case of two-bit address (N=2). The label recognition circuit for N=2 consists of two-stage connection of QPRC modules in a tree structure as shown in Fig.20. The ID bit pulse and the first bit pulse of the address are incident in the input port 1 and 2, respectively. The four outputs from the QPRC are sent to the input port 1 of the second-stage QPRC modules. The second-bit pulse of the code is four times amplified and then divided into four pulses to be incident in the input ports 2 of the four QPRC modules. In order to perform the same processing as the first-stage QPRC module in the second-stage QPRC modules, the phase of the output signals from the first-stage QPRC module has to be adjusted since the phases of the outputs are not the same as those shown in Table 1. The phase shift circuit is employed to adjust the phase. The outputs of the phase shift circuit $E_{out}^{(i)\prime}$, (i=1,...,4) are written as

$$\begin{pmatrix} E_{out}^{(1)\prime} \\ E_{out}^{(2)\prime} \\ E_{out}^{(3)\prime} \\ E_{out}^{(4)\prime} \end{pmatrix} = \begin{pmatrix} e^{j\Delta\phi_1} & 0 & 0 & 0 \\ 0 & e^{j\Delta\phi_2} & 0 & 0 \\ 0 & 0 & e^{j\Delta\phi_3} & 0 \\ 0 & 0 & 0 & e^{j\Delta\phi_4} \end{pmatrix} \begin{pmatrix} E_{out}^{(1)} \\ E_{out}^{(2)} \\ E_{out}^{(3)} \\ E_{out}^{(4)} \end{pmatrix}, \tag{10}$$

where $\Delta\phi_1=0$, $\Delta\phi_2=\pi/4$, $\Delta\phi_3=3\pi/4$, and $\Delta\phi_4=\pi/2$.

Table 2 shows the amplitudes $E_{out}^{(i)\prime}$ after the phase shift circuit. The maximum output at each output ports can be regarded as an ID bit pulse for recognizing the second-bit pulse of the address. The output intensities from the sixteen output ports for label $(E_{in}^{(1)}, E_{in}^{(2)}, E_{in}^{(3)})$ =(1, 1, 1), are shown Fig.21. It is found from this result that the maximum output intensity of $|E_{out}^{(i)}|^2=1$ is obtained at only one output port, and the minimum output intensity of

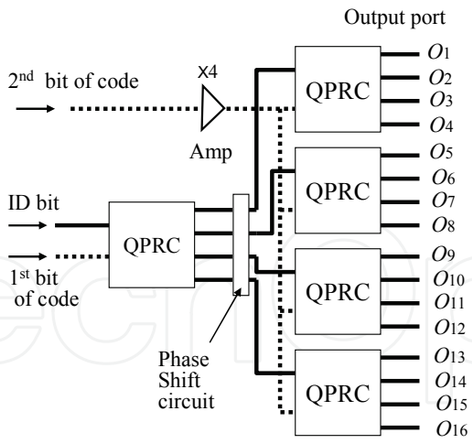

Fig. 20. Label recognition circuit for two-bit QPSK addresses.

Input phase ϕ_2	Output amplitude			
	$E_{out}^{(1)}$	$E_{out}^{(2)}$	$E_{out}^{(3)}$	$E_{out}^{(4)}$
0	$e^{j7\pi/4}/\sqrt{2}$	1	0	$e^{j\pi/4}/\sqrt{2}$
π	$e^{j\pi/4}/\sqrt{2}$	0	1	$e^{j7\pi/4}/\sqrt{2}$
π/2	1	$e^{j\pi/4}/\sqrt{2}$	$e^{j7\pi/4}/\sqrt{2}$	0
3π/2	0	$e^{j7\pi/4}/\sqrt{2}$	$-e^{j\pi/4}/\sqrt{2}$	1

Table 2. Electric field of the optical output after phase shift circuit.

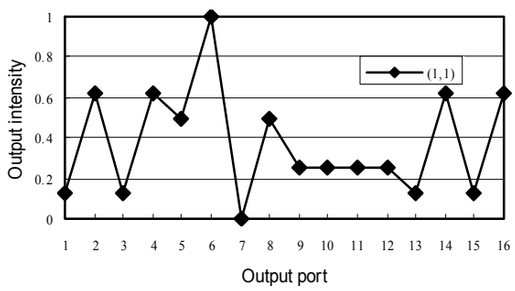

Fig. 21. Output intensities at sixteen output ports for input label $(E_{in}^{(1)}, E_{in}^{(2)}, E_{in}^{(3)}) = (1, 1, 1)$.

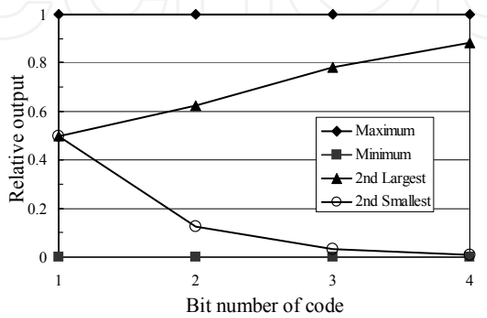

Fig. 22. Relative output intensities of the maximum, 2nd largest, 2nd smallest and minimum outputs.

$|E_{out}^{(i)}|^2=0$ only one of the other output ports. These output ports for $|E_{out}^{(i)}|^2=1$ and $|E_{out}^{(i)}|^2=0$ are different for all the sixteen addresses. The output intensities of the second largest and the second smallest output are 0.625 and 0.125, respectively. By employing threshold devices after the output ports, the output port of the maximum intensity or minimum intensity can be identified. Thus, two-bit QPSK addresses can be recognized with this circuit.

The number N of the code bit to be recognized can be increases by repeating the similar operation with increased stage number. We calculated the output intensities for three-bit (N=3) and four-bit (N=4) addresses. The output intensities corresponding to the maximum, the minimum, the second largest and the second smallest outputs for N=1 to N=4 are plotted in Fig.22. Although refined threshold devices will be required to recognize the addresses for $N > 3$, multiple-bit addresses are recognizable in principle.

7. Conclusion

Label recognition by interfering an identifying pulse with address pulses with integrated-optic circuits was discussed. All the addresses can be identified with a single circuit by self-routing manner. The circuits consist of passive devices such as asymmetric X-junction couplers, Y-junction dividers and directional couplers. Therefore, the circuits can be formed on various substrates. Since the wavelength dependence in these devices is small, the device can be used for optical labels at a wavelength in a wide wavelength range. Although the contrast ratio of the output from the port corresponding to the destination address and that from the other ports decreases as the bit number of the address increases, the contrast ratio can be improved by employing nonlinear post-processing devices such as thresholding devices.

8. References

Blumenthal, D. J; Olsson, B. E.; Rossi, G.; Dimmich, T. E.; Rau, L; Masanovic, M.; Lavrova, O; Doshi, R.; Jerphagnon, O.; Bowers, J. E.; Kaman, V.; Coldren, L. A. & Barton, J. (2000). All-Optical label swapping networks and technologies, J. Lightwave Technol., vol.18, no.12, pp.2058-2075, Dec.2000.

Burns, W. K. & Milton, A. F. (1975). Mode conversion in planar-dielectric separating waveguides, IEEE J. Quantum Electron., vol.QE-11, no.1, pp.32-39, Jan. 1975.

Burns, W. K. & Milton, A. F. (1980). An analytic solution for mode coupling in optical waveguide branches, IEEE J. Quantum Electron., vol.QE-16, no.4, pp.446-454, Apr. 1980.

Cincotti, G. (2004). Full optical encoders/decoders for photonic IP routers, J. Lightwave Technol., vol.22, no.2, pp.337-342, Feb. 2004.

Glesk, I.; Kang, K. I. & Prucnal, P. R. (1997). Ultrafast photonic packet switching with optical control, Optics Express, vol.1, no.5, pp.126-132, Sep. 1997.

Goto, N & Miyazaki, Y. (2005). Label recognition with wavelength-selective collinear acoustooptic switches for photonic label routers, Jpn. J. Appl. Phys., vol.44, no.6B, pp.4449-4454, June 2005.

Hiura, H. & Goto, N. (2005). Proposal of all-optical label recognition using self-routing circuits, Proc. Int. Quantum Electronics Conf. 2005 and the Pacific Rim Conf. on

Lasers and Electro-Optics 2005 (IQEC/CLEO-PR 2005), Tokyo, Japan, CFJ4-3, July 2005.

Hiura, H. & Goto, N. (2006). All-optical label recognition using tree-structure self-routing circuits consisting of asymmetric X-junctions, Proc. of Conf. on Lasers and Electro-Optics, and Quantum Electronics and Laser Science Conf. (CLEO/QELS) 2006, Long Beach, California, USA, JThC73, May 2006.

Hiura, H. & Goto, N. (2007a). All-optical label recognition using self-routing architecture of Mach-Zehnder interferometer optical switches with semiconductor optical amplifiers, IEICE Trans. Electron., vol.E90-C, no.8, pp.1619-1626, Aug. 2007.

Hiura. H; Narita, J. & Goto, N. (2007b). Optical label recognition using tree-structure self-routing circuits consisting of asymmetric X-junctions, IEICE Trans. Electron., vol.E90-C, no.12, pp.2270-2277, Dec. 2007.

Hiura, H.; Makimoto, Y.; Goto, N. & Yanagiya, S. (2008). Optical multiple-wavelength BPSK label recognition with self-touting waveguide-circuit, The 7th Int. Conf. on Optical Internet (COIN2008), Tokyo, Japan, C-16-PM1-2-5, Oct.2008.

Izutsu, M.; Enokihara, A. & Sueta, T. (1982). Optical-waveguide hybrid coupler, Opt. Lett., vol.7, no.11, pp.549-551, Nov.1982.

Kitayama, K.; Wada, N & Sotobayashi, H. (2000). Architectural considerations for photonic IP router based upon optical code correlation, J. Lightwave Technol., vol.18, no.12, pp.1834-1844, Dec.2000.

Kurumida, I.; Uenohara, H. & Kobayashi, K. (2006). All-optical label recognition for time-domain signal using multistage switching scheme based on SOA-MZIs, Electron. Lett., vol.42, no.23, pp.1362-1363, Nov. 2006.

Makimoto, Y; Hiura, H.; Goto, N. & Yanagiya, S. (2008). Proposal of waveguide-type optical circuit for recognition of optical QPSK coded labels in photonic router, OECC/ACOFT 2008, Sydney, ThK-1, July 2008.

Makimoto, Y; Hiura, H.; Goto, N. & Yanagiya, S. (2009a). Waveguide-type optical circuit for recognition of optical QPSK coded labels in photonic router, J. Lightwave Technology, Vol.27, No.1, pp.60-67, Jan. 2009.

Makimoto, Y.; Hiura, H.; Goto, N & Yanagiya, S. (2009b). Wavelength dependence of waveguide-type optical circuit for recognition of optical QPSK labels in photonic router, The 14th OptoElectronics and Communications Conference (OECC2009), Hong Kong, July 2009.

Moriwaki, O.; Kitoh, T.; Sakamoto, T. & Okada, A. (2005). Novel PLC-based optical correlator for multiple phase-modulated labels, IEEE Photon. Technol. Lett., vol.17, no.2, pp.489-491, Feb. 2005.

Renaudier, J.; Charlet, G.; Salsi, M.; Pardo, O. B.; Mardoyan, H.; Tran, P. & Bigo, S (2008) , Linear fiber impairments mitigation of 40-Gbit/s polarization-multiplexed QPSK by digital processing in a coherent receiver, J. Lightwave Technol., vol. 26, no.1, pp.36-42, Jan. 2008.

Seo, S. W.; Bergmann, K. & Prucnal, P. R. (1996) . Transparent optical networks with time-division multiplexing, J. Select. Areas Commun., vol.14, no. 6, pp.1039-1051, June 1996.

Takiguchi, K.; Shibata, T. & Itoh, M. (2002). Encoder/decoder on planar lightwave circuit for time-spreading/wavelength-hopping optical CDMA, Electron. Lett., vol.38, no.10, pp.469-470, May 2002.

Teh, P. –C.; Petropoulos, P.; Ibsen, M. & Richardson, D. J. (2001). A comparative study of the performance of seven- and 63 chip optical code-division multiple-access encoders and decoders based on superstructured fiber Bragg gratings, J. Lightwave Technol., vol.19, no.9, pp.1352-1365, Sep. 2001.

Wada, N & Kitayama, K. (1999). A 10 Gb/s optical code division multiplexing using 8-chip optical bipolar code and coherent detection, J. Lightwave Technol., vol.17, no.10, pp.1758-1765, Oct. 1999.

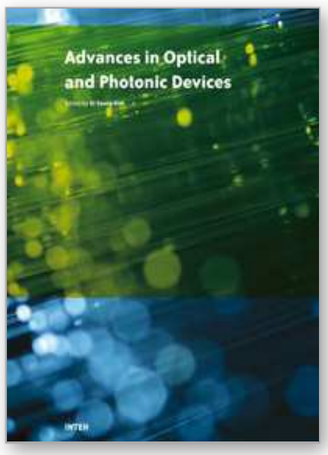

Advances in Optical and Photonic Devices

Edited by Ki Young Kim

ISBN 978-953-7619-76-3
Hard cover, 352 pages
Publisher InTech
Published online 01, January, 2010
Published in print edition January, 2010

The title of this book, Advances in Optical and Photonic Devices, encompasses a broad range of theory and applications which are of interest for diverse classes of optical and photonic devices. Unquestionably, recent successful achievements in modern optical communications and multifunctional systems have been accomplished based on composing “building blocks” of a variety of optical and photonic devices. Thus, the grasp of current trends and needs in device technology would be useful for further development of such a range of relative applications. The book is going to be a collection of contemporary researches and developments of various devices and structures in the area of optics and photonics. It is composed of 17 excellent chapters covering fundamental theory, physical operation mechanisms, fabrication and measurement techniques, and application examples. Besides, it contains comprehensive reviews of recent trends and advancements in the field. First six chapters are especially focused on diverse aspects of recent developments of lasers and related technologies, while the later chapters deal with various optical and photonic devices including waveguides, filters, oscillators, isolators, photodiodes, photomultipliers, microcavities, and so on. Although the book is a collected edition of specific technological issues, I strongly believe that the readers can obtain generous and overall ideas and knowledge of the state-of-the-art technologies in optical and photonic devices. Lastly, special words of thanks should go to all the scientists and engineers who have devoted a great deal of time to writing excellent chapters in this book.

How to reference

In order to correctly reference this scholarly work, feel free to copy and paste the following:

Nobuo Goto, Hitoshi Hiura, Yoshihiro Makimoto and Shin-ichiro Yanagiya (2010). Integrated-Optic Circuits for Recognition of Photonic Routing Labels, Advances in Optical and Photonic Devices, Ki Young Kim (Ed.), ISBN: 978-953-7619-76-3, InTech, Available from: http://www.intechopen.com/books/advances-in-optical-and-photonic-devices/integrated-optic-circuits-for-recognition-of-photonic-routing-labels

INTECH
open science | open minds

InTech Europe
University Campus STeP Ri
Slavka Krautzeka 83/A
51000 Rijeka, Croatia
Phone: +385 (51) 770 447

InTech China
Unit 405, Office Block, Hotel Equatorial Shanghai
No.65, Yan An Road (West), Shanghai, 200040, China
中国上海市延安西路65号上海国际贵都大饭店办公楼405单元
Phone: +86-21-62489820

Fax: +385 (51) 686 166
www.intechopen.com

Fax: +86-21-62489821

IntechOpen